CrossMark

R. Lichtenthäler · M. A. G. Alvarez · A. Lépine-Szily ·
S. Appannababu · K. C. C. Pires · U. U. da Silva ·
V. Scarduelli · R. P. Condori · N. Deshmukh

RIBRAS: The Facility for Exotic Nuclei in Brazil

Abstract A description of the RIBRAS (radioactive ion beams in Brasil) facility is presented and the last experimental developments in the system are reported.

1 Introduction

Over the last few decades, the study of nuclei away from the stability line has been one of the major research areas in low energy nuclear physics. The research field is very extense and ranges from light and intermediate mass nuclei, which includes nuclei of astrophysical interest, up to the super-heavy elements. In the nuclear chart, far from stability, one can find the exotic nuclei, characterized by being proton or neutron rich elements, short-lived and rarely found in nature, some of them characterized by a halo structure.

The light neutron rich exotic nuclei, such as ^{6}He, ^{11}Li, ^{11}Be among others, present a pronounced cluster structure formed by a core plus one or two loosely bound neutrons and are examples of weakly bound systems. Their breakup energies are very small compared to the known stable nuclei, what modifies the way exotic nuclei interact, and their half-lifes are sufficiently long which allow the production of secondary beams, to perform scattering and reaction experiments.

Many laboratories in the world are dedicated to this research area. RIBRAS is a large acceptance double solenoid system to select low-energy secondary beams of nuclei away from the stability line. It is installed in the Open Laboratory of Nuclear Physics of the Institute of Physics of the University of São Paulo and is in operation since 2004 [1,2].

The driver accelerator is a 8UD-Pelletron which delivers primary beams of stable nuclei like ^{6,7}Li, ^{10,11}B in the energy range between 2 and 5 MeV/nucleon and with intensities of hundreds of electric nano-Amps. The secondary beam is produced in-flight, by nucleon transfer reactions between the primary beam and the primary target. The large acceptance of the solenoids (30 msr) combined with relatively large production cross sections permit RIBRAS to deliver secondary beams such as ^{6}He, ^{8}Li, ^{8}B, ^{7}Be with intensities around $10^4 - 10^6$ pps.

A large research program has been carried out in RIBRAS since 2004, mainly involving elastic scattering measurements of neutron rich nuclei like ^{6}He, ^{8}Li and proton rich nuclei like ^{7}Be, ^{8}B on secondary targets of different masses. The first experiments have been performed in the central scattering chamber using the first solenoid only. Since 2011 a new secondary scattering chamber was installed after the second solenoid allowing the use of the double solenoid system.
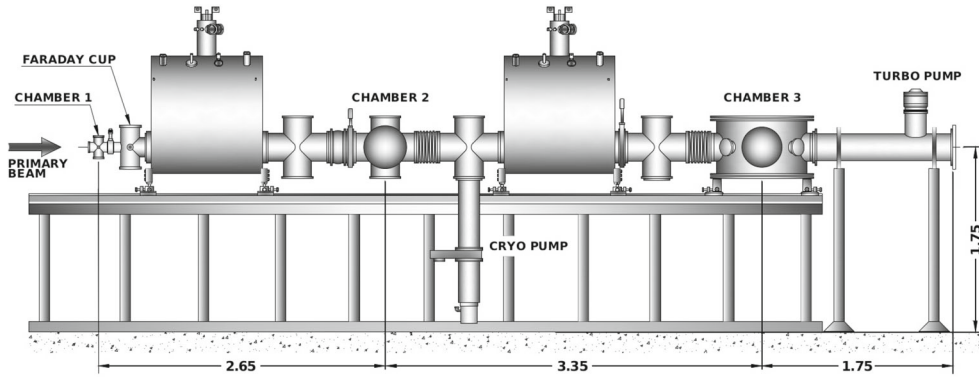
R. Lichtenthäler (✉) · M. A. G. Alvarez · A. Lépine-Szily · S. Appannababu · K. C. C. Pires · U. U. da Silva ·
V. Scarduelli · R. P. Condori · N. Deshmukh
Universidade de Sao Paulo, São Paulo, Brazil
E-mail: rubens@if.usp.br

Fig. 1 Schematic diagram of the RIBRAS facility. The primary target scattering chamber, ISO-250 central scattering chamber and the scattering chamber after the second solenoid are called chambers 1, 2 and 3 respectively

Table 1 Secondary beams produced at RIBRAS with production reactions, intensities, energy resolution/energy and purity in the scattering chamber 2

Secondary beam	Production reaction	Q-value (MeV)	Intensity (pps)	Energy resolution FWHM (keV)/Energy	Purity %
^{6}He	^{9}Be(^{7}Li,^{6}He)^{10}B	−3.390	10^5–10^6	1000/22 MeV	16
^{7}Be	^{3}He(^{6}Li,^{7}Be)d	+0.112	10^4–10^5	800/18.8 MeV	2
^{7}Be	^{7}Li(^{6}Li,^{7}Be)^{6}He	−4.369	10^4–10^5	1000/22 MeV	2
^{8}Li	^{9}Be(^{7}Li,^{8}Li)^{8}Be	+0.367	10^5–10^6	500/25.8 MeV	44
^{8}B	^{3}He(^{6}Li,^{8}B)n	−1.975	10^4	1000/15.6 MeV	4.4
^{10}Be	^{9}Be(^{11}B,^{10}Be)^{10}B	−4.642	10^5	800/23.2 MeV	3
^{12}B	^{9}Be(^{11}B,^{12}B)^{8}Be	+1.705	10^5	800/25.0 MeV	

2 The RIBRAS System

The current RIBRAS setup is shown in Fig. 1. The secondary particles are produced by nuclear reactions between the primary beam and the primary target located in the primary scattering chamber (chamber 1), usually nucleon transfer or fusion evaporation reactions. After crossing the primary target, the primary beam is suppressed in the Faraday cup and its current can be integrated allowing an on-line measurement of the number of incident particles impinging on the primary target. The acceptance cone of the first solenoid ($2° \leq \theta \leq 6°$) is defined by the Faraday cup and a collimator located just before the first solenoid. The first solenoid makes an in-flight selection of the secondary beam, focusing the particles with the same magnetic rigidity ($B\rho$) in the central scattering chamber (chamber 2). Table 1 shows a list of the secondary beams produced so far in RIBRAS [2].

The secondary beam in the scattering chamber 2 is usually contaminated by particles with the same magnetic rigidity but different masses, charge states and energies. Contaminations come mainly from the degraded primary beam but also from light particles such as alphas, deuterons and protons which are produced by reactions in the primary target. These unwanted particles can be suppressed by using blockers and collimators strategically positioned along the solenoid beam line.

In Fig. 2 we show a $\Delta E - E$ spectrum recently obtained in chamber 2. ^{7}Li(^{6}Li,^{7}Be)^{6}He was the primary reaction used to produce the ^{7}Be secondary beam.

A degrader can be used in chamber 2 to allow an additional charge exchange and differential energy loss with subsequent filtering by the second solenoid. An improvement in the secondary beam purity up to about 99 % is obtained in some cases.

In Fig. 3 two $\Delta E - E$ spectra are shown both in chamber 3 without and with degrader in chamber 2, for the ^{9}Be(^{7}Li,^{8}Li)^{8}Be primary reaction.

The (70 cm diameter × 40 cm height) scattering chamber (chamber 3) located after the second solenoid has a system of two independent plates (see Fig. 4). The movement of the plates is remotely controlled by two step motors and the measurement of the scattering angles is done using the signals from reference sensors located under the plates. This system allows the measurement of angular distributions and experiments in kinematic
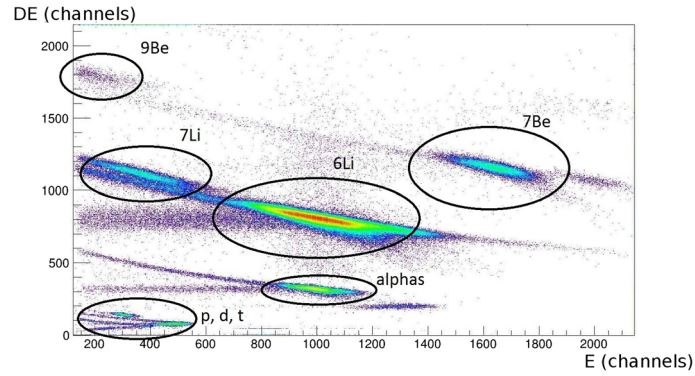
Fig. 2 $\Delta E - E$ spectrum for a ^{7}Be secondary beam scattered at $\theta_{lab} = 65°$ on a ^{197}Au target. Taken in scattering chamber 2
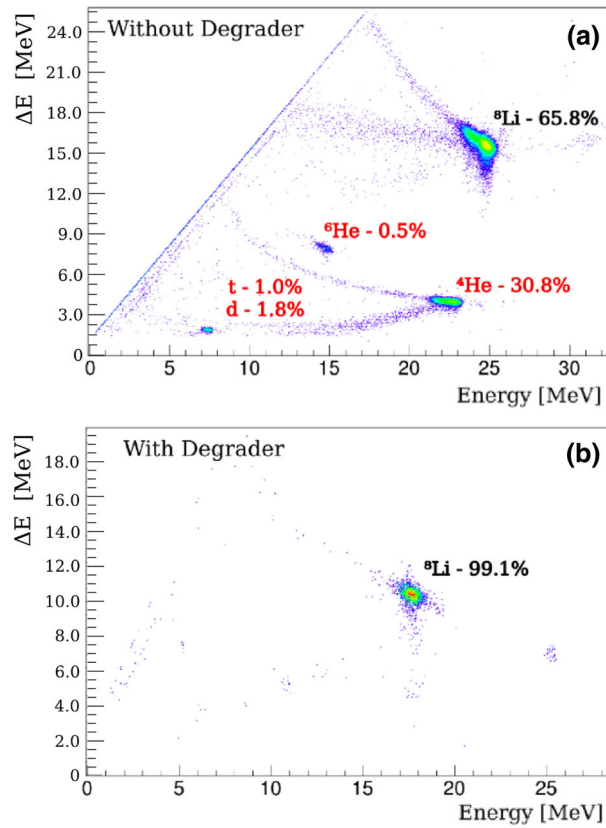

Fig. 3 $\Delta E - E$ spectra for a ^{8}Li secondary beam before and after cleaning up by the use of a degrader in chamber 2. Figure taken from Ref. [2]

coincidences. Kinematic coincidence is a useful technique to separate and identify certain kinds of reactions and can be applied in RIBRAS using detectors with large solid angles.

3 Research Program at RIBRAS.

The research program developed at RIBRAS consisted mostly of elastic scattering measurements with light exotic nuclei on targets of several masses. Elastic scattering angular distributions provide information about the nuclear potential as well as of the total reaction cross section.
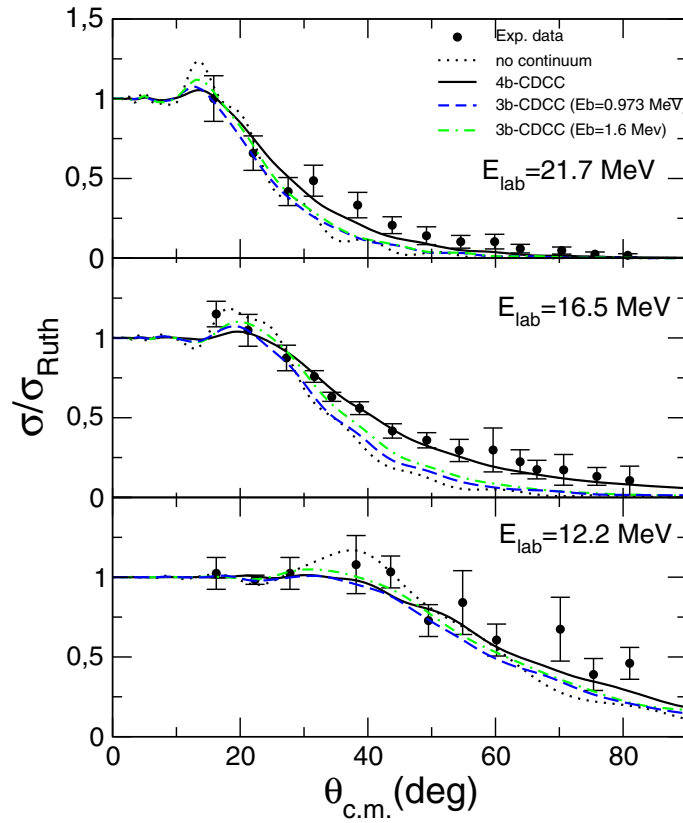
Fig. 4 Secondary scattering chamber

Fig. 5 ^{6}He+^{58}Ni elastic angular distributions measured at RIBRAS [10]

At low energies the elastic angular distributions are affected by both the long range Coulomb and the short range nuclear interactions and the measurement of elastic scattering angular distributions on different mass targets allows the study of the interplay between Coulomb and nuclear interactions [3,4].

Elastic scattering of ^{6}He, ^{8}Li and ^{7}Be on ^{9}Be, ^{12}C, ^{27}Al, ^{58}Ni and ^{120}Sn has been investigated in RIBRAS [5–11].

The angular distributions have been analysed by different theoretical models such as Optical Model, Coupled Channels as well as the state-of-the-art three and four-body Continuum Discretized Coupled Channels (CDCC) calculations. As an example we show in Fig. 5 three ^{6}He+^{58}Ni angular distributions compared with
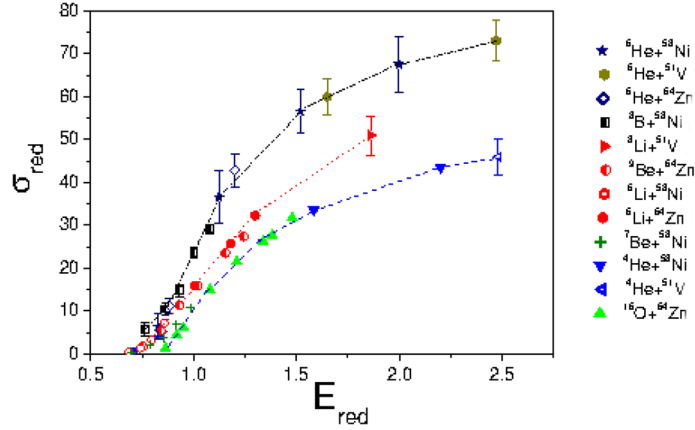
Fig. 6 Systematics of the total reaction cross section for stable, weakly bound and exotic projectiles on $A \approx 60$ targets where $E_{red} = E_{cm}(MeV) \times (A_p^{1/3} + A_t^{1/3})/Z_p Z_t$ and $\sigma_{red} = \sigma_{reac}(mb)/(A_p^{1/3} + A_t^{1/3})^2$ [2]
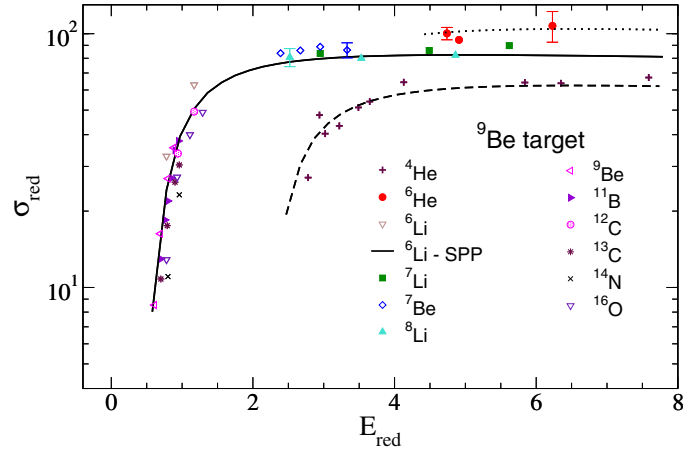

Fig. 7 Systematics of the total reaction cross section for stable, weakly bound and exotic projectiles on ^{9}Be target [13]

three and four-body CDCC calculations. We remark the enhancement effect, with respect to the 3b-CDCC calculations, in the cross sections observed at intermediate angles, which is well reproduced by the 4b-CDCC without any free parameter.

The total reaction cross sections have been obtained from these analysis and a comparison of the reduced total reaction cross sections for exotic and stable systems has been performed, showing that, for ^{6}He on heavy and intermediate mass targets such as ^{58}Ni [2,10] and ^{120}Sn [11,12] there is an enhancement of about 50 % in the total reaction cross sections compared to other isobar weakly bound stable projectiles ^{6,7}Li and ^{9}Be (see Fig. 6). However, as we go to lighter targets such as ^{9}Be this enhancement is reduced to about 20 % (see Fig. 7).

In addition to the elastic scattering angular distribution measurements we are developing a program of resonant reactions measurements using the thick target method. Proton rich plastics such polyethylene (CH_2) foils have been used as targets to study fusion-evaporation reactions such as p(^{6}He,p)^{6}He, p(^{6}He,α)t, p(^{8}Li,p)^{8}Li and p(^{8}Li,d)^{7}Li. The CH_2 seconday targets are sufficiently thick to absorb most of the secondary beam energy but not the recoil light particles such as protons, deuterons and alphas which are detected in the forward angles. The energy spectra of the light particles detected at forward angle provide a measurement of the excitation functions of fusion-evaporation reactions at backward center of mass angles. The presence of peaks in the spectra is related to resonances in the compound system. This technique allows spectrocopic studies of light nuclei like ^{7}Li and ^{9}Be at relatively high excitation energies [14,15]. Contaminant reactions in the Carbon of the CH_2 target can be subtracted by measurements using a pure Carbon target and the presence of contaminations in the secondary beam can be monitored using a pure Gold target, where just scattering (no reactions) takes place.
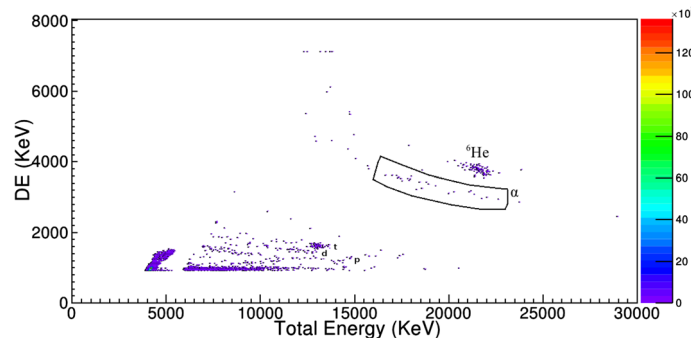
Fig. 8 $\Delta E - E$ spectrum for the ^{120}Sn(^{6}He,α)X reaction at $\theta_{lab} = 36°$

4 Recent Results and Future Developments

The extension of the RIBRAS capabilities beyond elastic scattering measurements will require both, improvements in the purity of the secondary beams and developments in the detection system to permit a more selective identification of the reaction products. One of these improvements is the use of a pulsed primary beam which is presently under development in the laboratory. Pulsed primary beams plus time of flight measurements allow the identification of the secondary beam particles and the tagging of events produced in coincidence with the secondary particles of interest.

The use of segmented solid state detectors such as CD's and S/DSSSD's (Single/Double Sided Silicon Strip Detectors) enhances the efficiency of angular distribution measurements. In addition, the detection of neutrons and particle-gamma coincidence measurements would enhance the reaction selectivity of the system.

An extension of the RIBRAS beam line was recently installed after chamber 3, to be connected with a gamma-particle cave shielded by a wall of boron-loaded water to allow the use of gamma detectors in a low neutron background environment. The entire setup has to be mounted in a region far from the primary target to avoid the large yield of secondary neutrons produced by reactions in the primary target, which could damage the Ge-Li detectors. A project for the instalation of this new scattering chamber for gamma-particle coincidences is in progress. It will consist of a small scattering chamber with four large area $\Delta E-E$ silicon telescopes to detect particles, surrounded by two HPGe detectors to detect gammas in coincidence. The chamber will be located in the end of the present beam line. The center of chamber 3 is located at 5.8 m from the primary target and the gamma-particle chamber will be mounted at 8.0 m (Fig. 1). In this position the secondary beam spot will be larger than at the actual RIBRAS secondary chamber position due to the magnifying effect of the second solenoid. We performed calculations of the RIBRAS beam profile using a Monte-Carlo simulation code developed by E. Leistenschneider [16] and we found that the beam spot size has a diameter of about 10 mm at 8.0 m, what makes the experiment feasible in principle.

Recently we performed new measurements of the ^{120}Sn(^{6}He,α)X reaction at $E_l = 22.5$ MeV in the secondary scattering chamber. A large yield of alpha particles was observed at intermediate angles, between $30° \le \theta \le 70°$, which are probably produced in neutron transfer reactions (see Fig. 8). The measured alpha particle production cross sections in this experiment are around $\sigma_\alpha = 400$ millibarns. It is in agreement with the previous measurements at slightly lower energies [17]. This is a quite large cross section compared to the usual nucleon transfer or breakup cross sections involving stable nuclei, which are of the order of tens of millibarns. The identification of the alpha particle production mechanism is a challenge and requires the measurement of additional observables such as gamma-particle and neutrons in coincidence.

References

1. Lichtenthäler, R. et al.: Radioactive ion beams in Brazil (RIBRAS). Eur. Phys. J. A **25**, 733 (2005)

2. Lépine-Szily, A., Lichtenthäler, R., Guimarães, V.: The Radioactive ion Beams in Brazil (RIBRAS) facility. Eur. Phys. J. A **50**, 128 (2014)
3. Fernández-García, J.P., Alvarez, M.A.G., Chamon, L.C.: Investigation of Coulomb dipole polarization effects on reactions involving exotic nuclei. Phys. Rev. C **92**, 014604 (2015)
4. Lichtenthäler, R., Pampa-Condori, R., Pires, K.C.C.: Elastic scattering of neutron halo projectiles. Few-Body Syst. doi:10.1007/s00601-015-0987-7
5. Pires, K.C.C. et al.: Experimental study of ^{6}He$+^9$Be elastic scattering at low energies. Phys. Rev. C **83**, 064603 (2011)
6. Camargo, O., Guimaraes, V., Lichtenthaler, R. et al.: The ^{9}Be(^{8}Li,^{9}Be)^{8}Li elastic-transfer reaction. Phys. Rev. C **78**, 034605 (2008)
7. Zamora, J.C. et al.: ^{7,9,10}Be elastic scattering and total reaction cross sections on a ^{12}C target. Phys. Rev. C **84**, 034611 (2011)
8. Zamora, J.C., Guimarães, V., Barioni, A., Lépine-Szily, A., Lichtenthäler, R., Faria, P.N.de , Mendes, D.R., Gasques, L.R., Shorto, J.M.B., Scarduelli, V. et al.: Elastic scattering and total reaction cross sections for the ^{8}B,^{7}Be, and ^{6}Li$+^{12}$C systems. Phys. Rev. C **84**, 034611 (2011)
9. Benjamim, E.A. et al.: Elastic scattering and total reaction cross section for the ^{6}He$+^{27}$Al system. Phys. Lett. B **647**, 30 (2007)
10. Morcelle, V. et al.: Four-body effects in the ^{6}He$+^{58}$Ni scattering. Phys. Lett. B **732**, 228 (2014)
11. Faria, P.N. et al.: Elastic scattering and total reaction cross section of ^{6}He$+^{120}$Sn. Phys. Rev. C **81**, 044605 (2010)
12. Mohr, P. et al.: Comparison of ^{120}Sn(^{6}He,^{6}He)^{120}Sn and ^{120}Sn(a,a)^{120}Sn elastic scattering and signatures of the ^{6}He neutron halo in the optical potential. Phys. Rev. C **82**, 044606 (2010)
13. Pires, K.C.C., Lichtenthler, R., Lépine-Szily, A., Morcelle, V.: Total reaction cross section for the ^{6}He$+^9$Be system. Phys. Rev. C **90**, 027605 (2014)
14. Lichtenthäler, R., Condori, R.P., de Faria, P.N., Lépine-Szily, A., Mendes, Jr., D.R., Pires, K.C.C., Morais, M.C., Leistenschneider, E., Scarduelli, V., Shorto, J.M.B.: First Experiment with the Double Solenoid RIBRAS System. Vol. **1529** of AIP Conference Proceedings, pp. 197–201 (2013)
15. Mendes, D.R., Lépine-Szily, A., Descouvemont, P., Lichtenthäler, R., Guimarães, V., Faria, P.N.de , Barioni, A., Pires, K.C.C., Morcelle, V., Pampa Condori, R. et al.: The ^{8}Li(p,a)^{5}He reaction at low energies, and ^{9}Be spectroscopy around the proton threshold. Phys. Rev. C **86**, 064321 (2012)
16. Leistenschneider, E., Lépine-Szily, A., Lichtenthäler, R.: SIM-RIBRAS: a Monte-Carlo simulation package for RIBRAS system. In: XXXV Brazilian Workshop on Nuclear Physics, vol. 1529, pp. 206–208. AIP, São Sebastião, São Paulo (2013). doi:10.1063/1.4804118
17. Faria, P.N. et al.: α-particle production in ^{6}He$+^{120}$Sn collisions. Phys. Rev. C **82**, 034602 (2010)